

Reports

Density Distribution in Earth

Abstract. Earth models selected by a Monte Carlo procedure were tested against geophysical data; 5 million models were examined and six have passed all tests. Common features of successful models are an increased core radius and a chemically inhomogeneous core consistent with Fe-Ni alloy (20 to 50 percent Fe) for the solid portion and Fe-Si alloy (15 to 25 percent Fe) for the fluid core. The inhomogeneous mantle is consistent with an increase in the FeO:FeO + MgO ratio by a factor of 2 in the deep mantle. The transition zone is a region of not only phase change but also composition change; this condition would inhibit mantle-wide convection. The upper-mantle solutions show large fluctuations in density; this state implies insufficient constraint on solutions for this region, or lateral variations in mantle composition ranging from pyrolyte to eclogite.

Most discussions of the internal density distribution in Earth make one or more of the following assumptions:

1) Large segments of the mantle (except the transition zone at depths of 400 to 1000 km) are homogeneous, adiabatic, or slightly superadiabatic and hydrostatic.

2) An initial density distribution corresponding to a specific composition is proposed for the upper mantle, primarily based on petrological arguments.

3) Density is related to seismic velocities through an empirical equation-of-state derived from laboratory measurements on minerals and rocks (1-3).

These assumptions have varying degrees of plausibility, but the possibility is real that Earth behaves differently. Here I derive density distributions independent of the above assumptions. My approach is by use of a Monte Carlo

method (4) in which Earth models are randomly generated; each consists of a compressional-velocity, shear-velocity, and density distribution in the mantle, determined randomly but required to lie between certain upper and lower limits.

The core densities also are selected randomly, as is the radius of the core within the range 3473 ± 25 km. Superadiabatic density gradients are not permitted in the core. The compressional velocity in the core is fixed according to a recent model (1, solution I). A spherically symmetric pseudo-crust is fixed from the weighted average of oceanic and continental crustal data. The ranges permitted for the randomly varying parameters are broader than the bounds formed by most earlier models.

The problem of establishing unique-

ness of Earth models derived from geophysical data is still unsolved; for this reason all models proposed for Earth have been somewhat in doubt (5-7). One advantage of the Monte Carlo method is that it finds a smaller number of solutions, satisfying the geophysical data, from a very large number of possible models. The degree to which the successful solutions agree (or disagree) is a rough measure of the precision to which Earth models can be specified with the currently available data. Furthermore, Monte Carlo procedures find models lacking bias stemming from "initial" models or other preconceived notions of Earth's structure.

Approximately 5 million Earth models were generated; each was tested against the mass of Earth (5.976×10^{27} g), dimensionless moment of inertia (0.3308), travel times of the seismic phases *P*, *PcP*, *S*, and *ScS* at six distances in the range 25 to 100 deg, and Earth eigenperiods for the free oscillation modes ${}_0S_0$, ${}_0S_2 - {}_0S_{48}$, ${}_0T_2 - {}_0T_{44}$, ${}_1S_2 - {}_1S_8$, and ${}_2S_7$. The travel times and eigenperiods were the latest available (8), and tolerances were assigned to each datum according to the scatter of the observations. In computing mass, moment of inertia, travel time, and eigenperiods, values of compressional and shear velocities and density were used at 88 points within Earth; only 23 of these points were randomly varied, and the remaining values were obtained by linear interpolation. The entire procedure would have been impossible without the newly available variational parameters that permit extremely rapid computation of eigenperiods by "table look-up" within the computer (9).

Of the 5 million models tested, six met all constraints; the density distributions for three of the six are shown in Figs. 1 and 2 together with the lower and upper bounds for which solutions were permitted. The other three resembled one found by Landisman *et al.* (10) in which a near-zero density gradient was found in the deep mantle; they were rejected as implausible.

If the vanishing density gradient is produced by superadiabatic temperature gradients, unacceptable temperatures are required for the core-mantle interface. If it is the result of a compositional change such as the depletion of iron, a concomitant increase in the seismic ratio ϕ (square of the bulk sound speed) should occur; this was not found in the models. Also in Figs. 1 and 2 is a standard model based on a recent proposal by Birch (1, solution I). Table

Table 1. Fundamental-mode eigenperiod residuals (computed minus observed) in seconds for different models. Model 14.21, included for excellent higher-mode fit, should be rejected because of large S_2 residual. Model number also refers to change in core radius. Root-mean-square residuals were used for groups of modes.

Modes	Model				
	19.65	14.21	22.43	18.12	Standard
S_0	-0.3	-3.8	-1.8	-4.9	0.8
S_2	4.8	-18.7	-10.2	3.5	-21.8
S_{2-10}	5.29	7.04	5.49	4.01	9.94
S_{11-20}	1.75	0.72	1.59	0.74	1.24
S_{21-35}	0.56	.26	1.10	.30	3.12
S_{36-48}	.34	.43	0.67	.35	2.58
S_{2-48}	2.48	3.11	2.61	1.81	4.92
T_2	-10.0	-7.7	-1.4	-2.1	-20.4
T_{2-10}	3.82	3.40	2.42	2.56	7.59
T_{11-20}	1.03	1.34	0.86	1.37	1.80
T_{21-35}	1.04	1.02	1.01	0.86	0.99
T_{36-44}	1.50	1.47	1.54	.88	1.88
T_{2-44}	2.04	1.91	1.50	1.49	3.73

1 gives the eigenperiod residuals for the models shown in Figs. 1 and 2.

I now discuss features of the successful models. Every successful model required an increase in the radius of Earth's core—the range being 18 to 22 km. Increases in core radius have been proposed (11, 12). My results contribute, not by establishing uniqueness of a larger core, but building the case for it by increasing the number of models tested by a factor of 10^5 to 10^6 .

Every successful model shows inner-core densities significantly higher than that of the standard model, the central densities varying between 13.3 and 13.7 g/cm^3 . From the shock-wave data of McQueen and Marsh (13) the central densities of pure iron and pure nickel cores would be about 13 and 14 g/cm^3 , respectively. Meteoritic iron contains about 5 to 20 percent Ni, which corresponds to central Earth densities of about 13.1 to 13.3 g/cm^3 . I conclude that inner-core compositions ranging between meteoritic iron and something like an Fe-Ni alloy, with 50 percent Fe, satisfy the data.

The initial densities at the top of the fluid core range between 9.4 and 10.0 g/cm^3 , the upper limit being close to that of the standard model. These values are 10 to 20 percent lower than the density of 11.2 g/cm^3 that pure iron would show at the corresponding pressure and a laboratory temperature of about 2000°C. My results accord with earlier suggestions that lighter elements such as silicon are alloyed with iron (1, 2, 14) in the outer core. Using the recent shock-compression data for iron-silicon alloys (15) I estimate that a fluid core containing 75 to 85 percent of iron (by weight) near the top would be consistent with these results. All models require chemical inhomogeneity for the overall core. The homogeneity of the outer core cannot be established from my results. In my procedure, control over core densities comes indirectly from the eigenperiods only when the additional constraints of mass and moment of inertia are placed on the solutions.

In the mantle below 1000 km the successful solutions show a surprisingly narrow spread within the permitted range. Two of the three solutions are quite similar to the standard solution that Birch interprets as being consistent with a mixture of high-pressure oxides behaving adiabatically and with iron content constant throughout the lower mantle. The third solution (model 18.12) shows a reduced density gradient in the lower mantle, which could be accounted

for by a superadiabatic temperature gradient of about 2°C/km .

The transition zone at depths of 400 to 1000 km has long been recognized as a region of high density and velocity gradients in which phase changes occur. Solutions in this region typically have been based on assumed equations of state or on arbitrary patches between upper and lower mantle solutions. Without any of these assumptions my results show the transition zone as exhibiting even higher density gradients than does the standard model; I interpret this fact as implying a localization of high density gradients corresponding to marked phase transitions as well as changes in composition. Recent array studies of the slopes of P -wave travel-time curves show high velocity gradients

at about 400 and 700 km; these have been interpreted as the olivine-spinel transition and the transition from spinel to a mix of closely packed oxides (FeO , MgO , SiO_2 , Al_2O_3 , and such) (16, 17). Still open are the questions of whether other transitions occur, and how the transitions vary laterally.

The question of compositional homogeneity between the upper and lower mantle is important not only for its geochemical implications but also for its pertinence to the problem of mantle convection. A compositional change is stabilizing with respect to convection, and large-scale convection of the mantle would be inhibited. D. L. Anderson (18) recently proposed an equation-of-state relating density ρ , mean atomic weight \bar{M} , and seismic ratio ϕ , based on static

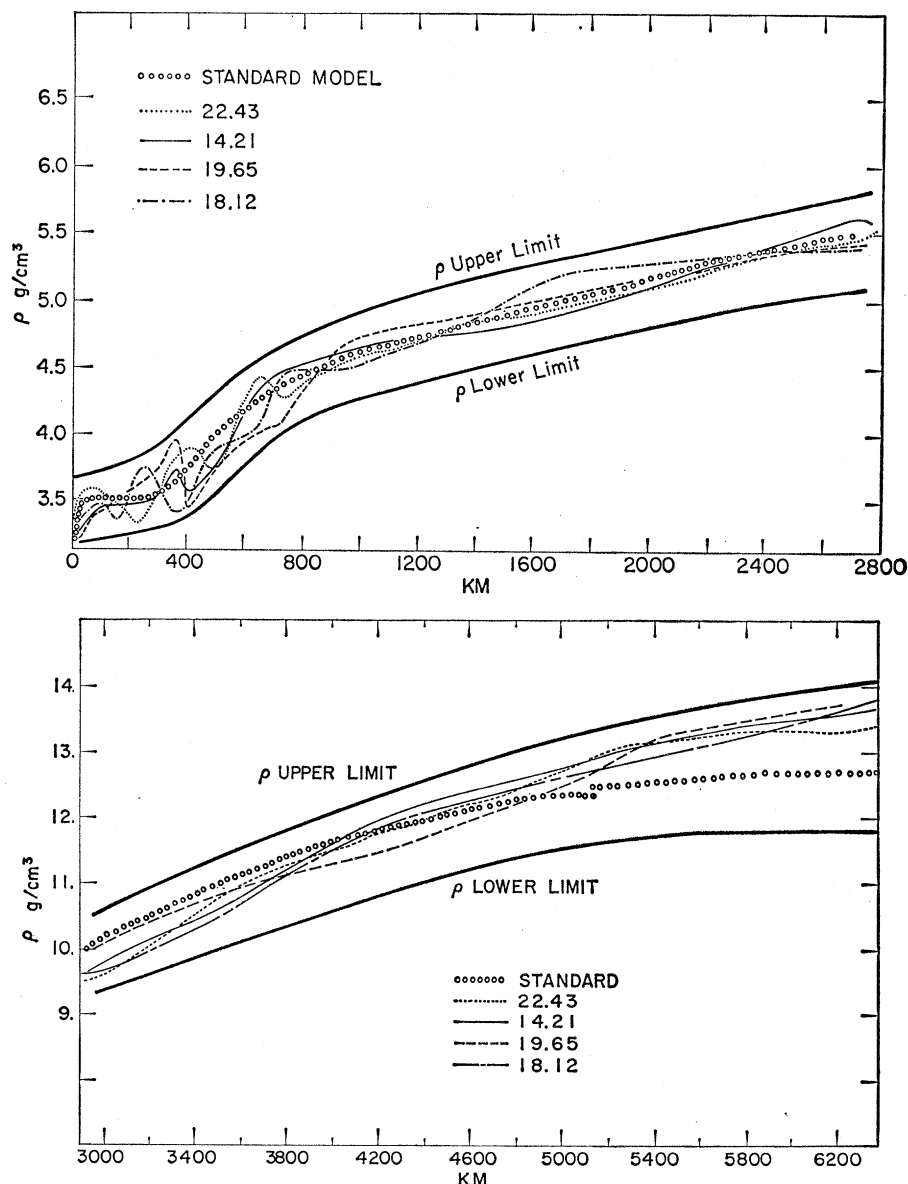
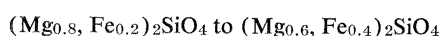


Fig. 1 (top). Density distributions in the mantle; successful models compared with standard model. Model number refers to increase in core radius in kilometers. Model 14.21, rejected because of large S_2 residual, is of interest because of small residuals for higher modes. Fig. 2 (bottom). Density distributions in the core.

compression and shock data for 31 oxide minerals and rocks with $18.6 < \bar{M} < 33.08$:

$$\rho/\bar{M} = 0.048\phi^{0.323} \quad (1)$$

I use Eq. 1 only as a convenient summary of currently available laboratory data, and I shall interpret changes in \bar{M} only in terms of changes in the Fe : Mg ratio. From my solutions and Eq. 1 I obtain an average value of \bar{M} for each of the two regions 33 to 370 km and 971 to 2796 km. For the upper mantle the permissible range was $19.8 \leq \bar{M} \leq 24.4$, and the solutions gave $22.0 \leq \bar{M} \leq 22.8$. For the lower mantle, the permissible range was $22.0 \leq \bar{M} \leq 26.3$, and the solutions gave $23.8 \leq \bar{M} \leq 24.6$. The difference $\Delta\bar{M}$ for the upper and lower mantles is given by $1.8 \leq \Delta\bar{M} \leq 2.3$, out of a possible range $-2.4 \leq \Delta\bar{M} \leq 6.5$. Although chemical homogeneity was permitted, all my solutions required an increase in \bar{M} for the lower mantle, but only when the entire lower mantle was averaged. My solutions do not require the composition change to be limited to the transition zone. One of Birch's density models, based on his P velocity-density relation and an a priori assumption that a change in $\Delta\bar{M}$ occurs, gave $\Delta\bar{M} = 1.9$ (19), although he also offered solutions in which the mantle was homogeneous. If we interpret variations in \bar{M} in terms of the equivalent FeO : FeO + MgO (molecular) ratio, our results imply a change in this ratio from about 0.2 to 0.4. The factor of 2 in the change is perhaps more significant than the actual values. For forsterite-fayalite solid solutions the corresponding change would be



D. L. Anderson (17) used an entirely different procedure in which array-determined P -velocities were compared with theoretical velocities for different forsterite:fayalite ratios. From his Fig. 5 one finds that the same composition change is required between the regions 200 to 350 km and 700 to 900 km in depth. In fact the indication of iron enrichment in the lower mantle does not depend on use of Eq. 1. If my solutions are plotted on a scatter diagram of laboratory determinations of bulk sound velocity ($\phi^{1/2}$) versus density for iron-magnesium silicates and oxides, the lower mantle solution is displaced toward the iron-enriched materials.

The successful models for the upper mantle (Fig. 1) show large variability, implying insufficient constraints on the solution with currently available geo-

physical data, at least so far as world averages are concerned. The models are complex, having one or two density minima, and show surprisingly large fluctuations in density. On the other hand, the standard model fits the eigenperiod data poorly (Table 1) even though it is simple by contrast and averages the successful models fairly well. This finding is especially true for the higher eigenvibration modes which are sensitive to upper-mantle structure. The better fit of the complex solutions points up the possibility that the upper mantle may be zoned vertically and horizontally to an extent not heretofore appreciated.

Below the rapid increase in density fixed by the M -discontinuity the solutions show initial mantle densities ranging from 3.34 to 3.54 g/cm³ out of a possible range of 3.18 to 3.60 g/cm³. The envelope of the upper-mantle density variations essentially covers the range between pyrolitic and eclogitic mantles. This result could indicate a lack of constraint on the solutions by the available data. I offer the hypothesis that the upper mantle is laterally and radially variable, and that large sections of an otherwise pyrolytic mantle are eclogitic. This situation could arise as follows: The primitive mantle is composed of pyrolite (density, 3.3 g/cm³) as proposed by Ringwood, the M -discontinuity being a compositional change. Fractional melting of pyrolite yields basaltic magma; some of the magma is extruded as lava during volcanic episodes, but large volumes may also be intruded at various levels in the upper mantle. Upon cooling, the intrusive basalts crystallize to eclogite, yielding a mantle having a density between 3.4 and 3.6 g/cm³, depending on the proportion of eclogite to pyrolite, temperature, and depth.

In many areas the transformation has not occurred, or a subsequent episode of fractional melting has transformed the eclogite to magma, giving densities lower than that of pyrolite. Thus the large fluctuations in density may be accounted for. This hypothesis differs from another (20) in requiring extensive zones of eclogite rather than small blocks. The mantle under midocean ridges and adjacent abyssal plains (well below the M -discontinuity) are candidate localities for intruded basalts and eclogites, respectively. The continental mantle is not exempt, however, since zones of high seismic velocity consistent with eclogitic composition (8.4 km/sec) have been found in the upper

mantle by refraction-profiling techniques (21).

Density fluctuations above the transition zone also may occur because of the separate or combined effects of temperature and pressure and mineral zoning. Green and Ringwood (22) predict two density minima in the upper mantle by these mechanisms, but the density variation is less than 1 or 2 percent, a quantity too small for detection.

Ibrahim and Nuttli (23) recently inverted new shear-wave travel-time data, including later arrivals, and found velocity minima involving reductions of the order of 10 percent almost exactly where the density minima of model 18.12 occur. By invocation of an additional constraint suggested by O. L. Anderson, this model could be given added weight; he used the Mie-Grüneisen equation-of-state to show that the signs of the shear-velocity and density gradients should be the same in a region of constant mean atomic weight (24). Only model 18.12 comes close to satisfying this criterion; furthermore it shows the two rapid increases in density in the transition zone which coincide almost exactly with the two compressional-velocity jumps found from array data (16, 17).

Using eigenmode data only, Gilbert and Backus (5) also found models having two minima in velocity and density. Bullen and Hadden (12), on the other hand, found Earth models lacking the complex upper-mantle features that I report. It is difficult to compare this last result with mine because the entire Jeffreys compressional-velocity distribution and the Jeffreys shear-velocity distribution in region D were retained; thus the model would not have passed the travel-time test.

The density reversals, if due to lateral or vertical variations (or both), imply unstable conditions. This implication is not unwarranted in view of the abundance of evidence of dynamic processes in the upper mantle, such as spreading of the sea floor, volcanism, seismic activity, variations in heat flow, large isostatic anomalies, and wandering of the poles.

My conclusions must be tempered by the possibility that, had I generated more than 5 million models, successful solutions may have been found differing significantly from those discussed here.

FRANK PRESS

Department of Geology and
Geophysics, Massachusetts Institute of
Technology, Cambridge 02139

References and Notes

1. F. Birch, *J. Geophys. Res.* **69**, 4377 (1964).
2. S. P. Clark, Jr., and A. E. Ringwood, *Rev. Geophys.* **2**, 35 (1964).
3. K. E. Bullen, *Geophys. J.* **7**, 584 (1963); E. C. Bullard, *Verhandel. Ned. Geol. Mijnbouwk. Genoot.* **18**, 23 (1957).
4. Monte Carlo procedures were first introduced in the U.S.S.R. to a more restricted class of inversion problems. V. I. Keilis-Borok and T. B. Yanovskaja, *Geophys. J.* **13**, 223 (1967) (summary of Soviet work); F. Press and S. Biehler, *J. Geophys. Res.* **69**, 2979 (1964).
5. F. Gilbert and G. E. Backus, *Bull. Seismol. Soc. Amer.*, in press; G. E. Backus and F. Gilbert, *Geophys. J.* **13**, 247 (1967).
6. I. J. Asbel, V. I. Keilis-Borok, T. B. Yanovskaja, *Geophys. J.* **11**, 25 (1966).
7. C. L. Pekeris, *ibid.*, p. 85.
8. For observed eigenperiods we use the tabulation by Pekeris (7). Travel times are based on H. A. Doyle and A. L. Hales, "The analysis of S waves to North American stations in the distance range 28°–82°," unpublished; S. D. Kogan, *Bull. Acad. Sci. USSR Geophys. Ser. 3 English Transl.* **1960**, 246 (1960); D. S. Carder, D. W. Gordon, J. N. Jordan, *Bull. Seismol. Soc. Amer.* **56**, 815 (1966).
9. R. Wiggins, *Physics of the Earth and Planetary Interiors*, in press. I thank Wiggins for use of his results before publication.
10. M. Landisman, Y. Sato, J. Nafe, *Geophys. J.* **9**, 439 (1965).
11. For example: J. Dorman, J. Ewing, L. E. Alsop, *Proc. Nat. Acad. Sci. U.S.* **54**, 364 (1965).
12. K. E. Bullen and R. A. W. Hadden, *ibid.* **58**, 846 (1967).
13. R. G. McQueen and S. P. Marsh, *J. Geophys. Res.* **71**, 1751 (1966).
14. A. E. Ringwood, *Geochim. Cosmochim. Acta* **15**, 257 (1959); L. Knopoff and G. J. F. MacDonald, *Geophys. J.* **3**, 68 (1960); D. L. Anderson, in *The Earth's Mantle*, T. F. Gaskell, Ed. (Academic Press, London, 1967), p. 355.
15. A. S. Balchan and G. R. Cowan, *J. Geophys. Res.* **71**, 3577 (1966).
16. L. R. Johnson, *ibid.* **72**, 6309 (1967); H. Kanamori, *Bull. Earthquake Res. Inst. Tokyo Univ.*, in press; H. Fujisawa, *Tech. Rep. ISSP Tokyo Univ. Ser. A* **272** (1967), p. 1.
17. D. L. Anderson, *Science* **157**, 1165 (1967).
18. ———, *Geophys. J.* **13**, 9 (1967).
19. F. Birch, *ibid.* **4**, 295 (1961).
20. A. E. Ringwood and D. H. Green, *Tectonophysics* **3**, 383 (1966).
21. For example: J. V. Pomerantseva, A. N. Moszhenko, G. V. Egorkina, J. A. Sokolova, in *Assoc. European Seismol. Comm. 9th* (Geophys. Inst., Copenhagen Univ., 1967), p. 43.
22. D. H. Green and A. E. Ringwood, *Earth Planetary Sci. Letters* **3**, 151 (1967).
23. A. K. Ibrahim and O. W. Nuttli, *Bull. Seismol. Soc. Amer.* **57**, 1063 (1967).
24. O. L. Anderson, *J. Geophys. Res.* **70**, 1457 (1965).
25. Supported by NASA grant NGR 22-009-123. I benefited from discussions with R. Wiggins, M. N. Toksoz, K. Aki, A. E. Ringwood, D. Wones, G. Simmons, L. Pakiser, D. L. Anderson, and O. L. Anderson. I thank F. Gilbert, G. E. Backus, R. Wiggins, A. E. Ringwood, O. L. Anderson, D. L. Anderson, H. Kanamori, H. Fujisawa, H. A. Doyle, and A. L. Hales for preprints. Joel Karnofsky was an invaluable assistant in the early stages.

1 March 1968

Paleosalinity of Permian Nonmarine Deposits in Antarctica

Abstract. *Argillites of the Permian Mount Glossopteris Formation were analyzed for clay minerals, trace elements, and phosphate paleosalinity. Mainly degraded and stripped illites occur. The determined salinity range, 29 to 33 parts per mille is designated the "paleosalinity signature" of the formation. Analysis of trace elements supports phosphate paleosalinity determinations. Data from Leaiid-bearing beds indicate a salinity range of 30 to 31 parts per mille that persisted some 137 years. Subsequent increase to 33 parts per mille corresponded to termination of leaiid occupancy of the area. These findings confirm and extend Nelson's study of phosphate paleosalinity.*

During the austral summer of 1966–67 one of us (P.T.) made a microstratigraphic study of a very thin Permian fossiliferous zone in the Ohio Range, Antarctica (1). This zone, containing ribbed valves of the extinct branchiopod conchostracan genus *Leaiid*, is extremely restricted, being less than 1 m thick; because of faulting at both ends it is traceable laterally for about 30 m (2). Most samples analyzed by us came from this zone.

Contents of Al-PO₄, Fe-PO₄, and Ca-PO₄ were selectively extracted from shales (3) and determined spectrophotometrically. The trace-element analysis of raw samples was done with a Jarrel Ash 1.5-m Wadsworth spectrograph. Quantitative values were determined from photographic plates, measured with a densitometer. Oriented, nonoriented, and glycolated samples were used for x-ray diffraction analysis (4).

Studies of trace elements involved

analysis of boron versus gallium and of boron versus vanadium (Fig. 1), as well as of boron alone (5). Regarding the analysis of boron alone, it has been shown that argillaceous rock containing 50 parts per million (ppm) of boron is probably of marine origin; less than 50 ppm suggests freshwater conditions at the time of deposition. Only sample 12 contained less than 50 ppm; the remaining samples were very close to the freshwater-marine boundary. In the boron-versus-gallium partition of samples, a freshwater trend is apparent (Fig. 1), while in the boron-versus-vanadium partition (Fig. 1), as with boron alone, a marine trend occurs. Thus, while the dominant condition was marine, one or more samples indicated freshwater conditions, and several samples were close to the partition boundaries in each of three geochemical analyses.

Some anomalous trace-element results merit comment; they are consid-

ered minor since independent checks are available to resolve such anomalies. In boron versus vanadium (Fig. 1), for example, the rock analysis of sample 12 plots on the marine side, while, as noted above, in the analysis of boron alone, it plots on the freshwater side. Moreover, the rock analysis of sample 11 partitions as freshwater (Fig. 1, top), and in the analysis of boron versus gallium) but plotted for boron alone the sample partitions as marine. Both samples 11 and 12 have a phosphate salinity of 31 parts per mille (ppt) (Table 1); thus this sea-water salinity is clearly lower than normal.

Generally the geochemical partition of samples into freshwater and marine on the basis of trace-element analysis was found to provide an independent check of determinations of phosphate salinity; apart from a few anomalies, the agreement is good. Of the four refinements in methodology discussed in this report, this is the first (that is, corroborative geochemical analyses).

Data on trace elements become important in the light of the salinity tolerance of conchostracans; these are chiefly freshwater (and, to a lesser degree, brackish-water) forms today and apparently so since Carboniferous time (6). No living forms inhabit marine basins.

The leaiid beds have been interpreted as representing a pond environment in a swamp area (1). *Glossopteris* flora at several horizons (Mount Glossopteris Formation), and thin coals observed far to the southwest of the leaiid zone and closer to the base of Mercer Ridge, as well as a carbonized leaiid zone and sooty plant bands above it, are some of the features suggestive of swamp conditions. Long (7) interpreted the formation to be a broad floodplain deposit; our data are in agreement. Freshwater ponds formed on a floodplain swamp at the margins of the sea coast. The water of such ponds was either a mixture of freshwater and marine water, or relict seawater that permitted conchostracan occupancy when it became less saline. We determined the clay mineralogy and phosphate paleosalinity of these beds also (3) (Table 1).

Illite is the chief mineral present, in a stripped or degraded form. (The variety of illite is determined by the characteristic shape and 2θ values of the x-ray diffractograms.) Table 1 shows that at station 0 [bed 021.13 (oldest) through bed 021.2 (youngest of the leaiid-bearing beds)] the dominant mineral is a mixed layer of illite and mont-